KERNFORSCHUNGSZENTRUM

KARLSRUHE

Juni 1968

KFK 790
EUR 3960 e

Institut für Reaktorentwicklung

Problems of Sodium Boiling in Fast Reactors

D. Smidt, P. Fette, W. Peppler, E.G. Schlechtendahl,
G.F. Schultheiss

GESELLSCHAFT FUR KERNFORSCHUNG M.B.H.

KARLSRUHE

KERNFORSCHUNGSZENTRUM KARLSRUHE

Juni 1968

KFK 790

EUR 3960 e

Institut für Reaktorentwicklung

Problems of Sodium Boiling in Fast Reactors *)

D.Smidt

P.Fette

W.Peppler

E.G.Schlechtendahl

G.F.Schultheiss

Gesellschaft für Kernforschung mbH.,Karlsruhe

*) Work performed within the association in the field of fast reactor development between the European Atomic Energy Community and Gesellschaft für Kernforschung mbH.,Karlsruhe

PROBLEMS OF SODIUM BOILING IN FAST REACTORS*)

D.Smidt, P.Fette, W.Peppler,
E.G.Schlechtendahl, G.F.Schultheiß

Institut für Reaktorentwicklung
Kernforschungszentrum Karlsruhe

1. Introduction

Interest in liquid metal boiling has been intensified by fast reactor safety considerations. The positive coolant void coefficient in connection with sodium boiling under certain circumstances may result in the destruction of the core.

From the safety standpoint the interest is concentrated on the following 3 questions:

a) In the case of boiling: How fast will the coolant be ejected from the channel? This leads to the input rate of reactivity into the core and the resulting destructive energy.

b) What degree of liquid superheat will be reached before boiling actually starts? This not only determines the ejection velocity during boiling, but also may be of importance with respect to the integrity of the core structure. The sudden flashing of superheated liquid results in a pressure pulse and it must be proven, that this may not deteriorate the neighbouring coolant channels.

c) Following the ejection a return flow of cold liquid (400 °C to 600 °C) into the empty channel may result in pressure pulses of the waterhammer type. This is defined as recondensation of some of the vapour volume and again may destroy the core structure.

---

*) Paper presented at the European Two-Phase Flow Meeting, Oslo, June 18 - 20, 1968

Therefore ejection, superheat and recondensation are the main safety aspects of sodium boiling. They differ to a certain extent from the classical fields of boiling and two-phase flow, namely heat transfer, fluid flow and pressure drop as well as boiling and hydrodynamic stability. On the other hand, the solution of the ejection problem will provide much better knowledge of bubble dynamics. The superheat problem leads into experimental and theoretical investigations on nucleation, effect of cavities in a very wetting liquid and from this side as a byproduct will also give a substantial contribution to the solution of boiling stability problems. This may not only deepen our insight into the fundamental problems but also have direct importance for other applications as for instance space technology.

For our field of interest, the boiling of sodium, the main difference with respect to water is not so much the large thermal conductivity or the high boiling temperature of sodium, but the larger surface tension (about a factor 2) and the smaller vapour-to-liquid density ratio (about a factor $\frac{1}{2}$). Therefore even for low qualities the void fraction is large and plug-type flow prevails. The large surface tension basically gives the same effect, that large bubbles energetically are preferred to small ones. Therefore to a large extent the behaviour of single bubbles is typical for sodium boiling dynamics.

2. Coolant Ejection

The dominating mechanisms of sodium ejection from a fast reactor fuel element are apparently quite well understood today. In earlier investigations homogeneous two-phase flow models which had originally been developed for boiling water, were initially applied to sodium [1,2,3,4] and further developed [5]. Calculations done with the TRANSFUGUE code [6] indicated that even with no superheat sodium boiling in heated channels tends to a separation of the liquid and the vapour phase. This tendency is emphasized if the liquid is significantly superheated. In [2] a piston model was proposed for single bubble growth calculations. The same model was employed in [7] and [8]. In [8] for the first time it was assumed that the heated surface is not completely blanketed with vapour, but rather that a liquid layer remains on the surface and that this layer constitutes the main source of vapour production. According to this model a digital code

("Blow") was developed for numerical analysis [9]. In this paper we shall describe a model which is based on the Blow-code but incorporates a number of significant improvements.

2.1 Model

Fig. 1 shows a simplified model of a coolant channel and indicates five important phases of bubble behaviour. In phase 1 there is no indication of bubble growth. If the heat input into the coolant exceeds the heat removal capability of the coolant, the coolant temperature will rise up to and even beyond the saturation temperature. The radius of stable gaseous nuclei which may exist in the bulk of the liquid or at the liquid-solid interface will be given by

$$p = p_s(T) - \frac{2\sigma}{R} + p_g \qquad (1)$$

with

p = liquid pressure near the nucleus
$p_s(T)$ = saturation pressure
p_g = partial gas pressure
σ = surface tension
R = nucleus radius
T = temperature of liquid-vapour interface

Here it was assumed that the partial pressure of the vapour in the nucleus is equal to the saturation pressure. This is justified according to [9]. With rising temperature one of the nuclei will approach the critical radius

$$r^{*} = \frac{p_s(T) - p}{2\sigma}, \qquad (2)$$

will become unstable and will grow into a bubble of approximately spherical shape. This is phase 2 of the bubble growth.

If the liquid was superheated to some degree the creation of the first bubble will cause a rapid pressure rise in its neighbourhood from pressure p to the saturation pressure $p_s(T)$. Thus any other nuclei which were approaching the critical size at pressure p will now become more sub-critical. Due to this "selfpressurization" the creation of more than one

bubble within a limited volume becomes more unlikely provided that the power input is not too high. This is particularly the case with sodium due to its excellent thermal conductivity and consequently the flat temperature distribution as compared to water. However, even if more than one bubble would start to grow at the same time, the overall behaviour would not be influenced significantly according to [10]. In our calculations we therefore assumed that there is only one bubble.

In order to describe the growth of the bubble in phase 2 we assumed that for bubble radius R smaller than the channel radius r

- the bubble is of spherical shape
- liquid motion around the bubble is irrotational
- the pressure p is constant at radius r

With these assumptions the dynamic behaviour of the bubble can be calculated [11]. It is

$$\frac{d^2R}{dt^2} = \frac{(p_B - p)r}{\rho R(r - R)} - \frac{1}{2}\left(\frac{dR}{dt}\right)^2 \cdot \left[\frac{3}{R} - \frac{r^2 + rR + R^2}{r^3}\right] \qquad (3)$$

with

t = time
p_B = pressure in the bubble less the surface tension effect
ρ = liquid density
R = bubble radius
r = channel radius
p = pressure at radius r

This equation together with the continuity condition and the two instationary Bernoulli-equations for the liquid upstream and downstream (see [9]) from the point of bubble nucleation provide a set of linear equations from which p and the acceleration of the liquid can be calculated.

After a very short time of acceleration (in the microsecond range for typical problems) the bubble radius grows at a constant rate while the dynamic behaviour is dominated by inertia of the liquid. Later, heat conduction from the bulk of the superheated liquid to the liquid-vapour interphase becomes the dominant phenomenon and the bubble growth rate decreases into a $r \sim \sqrt{t}$ behaviour [10,12].

Phase 3 of the bubble growth is reached when the bubble fills out the cross section of the channel. The shape of the bubble becomes cylindrical. The equations which describe the growth of the bubble were derived in [9]. While the existence of a liquid layer which remains on the heated surface is important, the exact thickness of this layer is only of minor interest during the ejection phase, because the vaporization of a very small quantity of liquid is sufficient to void the whole channel. Boiling and ejection experiments with liquid metal [13] and sodium-water-reaction studies [14] had indicated a layer thickness of several 0.1 mm. In Karlsruhe a series of tests was carried with ethanol. Fig. 2 shows a frame of a high speed movie which was taken from the growth of the bubble. The different reflection properties of wetted and dry portions of the heater rod indicate that a liquid layer was left in the heater and dries out while the bubble grows (dotted line = dry spot).

The thickness of the layer was determined according to the following assumptions:

1. Mass balance; (bubble volume growth during time of temperature holdup)

2. Energy balance; (from electrical power x time of temperature holdup)

3. Laminar sublayer thickness of the boundary layer [15]

Fig. 3 shows the coincidence of the results. Apparently the thickness of the laminar sublayer of the boundary layer is a good estimate of liquid layer thickness.

In the code (Blow 2) which was developed according to the model which was outlined here briefly, the axial and radial temperature distribution in the coolant channel and in the channel wall is described by 9 axial nodes in the coolant (one of which is the bubble) and 5 x 5 nodes in the channel wall. The reduction of the liquid layer thickness due to vaporization is taken into account in 5 layer nodes.

2.2 Results

The code Blow was checked against potassium boiling and ejection experiments carried out at Ispra [16]. Experimental measurement and

theoretical predictions of the dynamic bubble growth were found to be in good agreement [8]. The instant of bubble nucleation and the amount of superheat at the point of bubble nucleation were the two parameters which had to be varied to obtain a best fit. The variation of these parameters as compared to the measured values lies still within the measurement tolerances. It was found that the agreement improved with increasing superheat. The reason is that at high superheat values the superheated liquid itself contains sufficient excess energy for the generation of large amounts of vapour at high pressure in a short time, while at lower superheat the heat flux from the heater into the liquid and hence the temperature distribution within the liquid becomes more important. This is emphasized by the results of bubble growth calculations in a typical sodium cooled fast reactor geometry. Fig. 4 and 5 show the axial bubble growth starting at the center of the core for different fuel temperatures (i.e. heat fluxes). Fig. 4 indicates that a low superheat (20°C) there is significant influence of the heat flux, while this influence is negligible at high superheat (220 °C) as shown on Fig. 5.

Cross-checking of the more refined code Blow 2 with experiments is still under way. First comparisons with ejection simulation experiments with water (see par. 5.1) indicated good agreement for both the spherical and the cylindrical phase of bubble growth. Fig. 6 shows the radius of the spherical bubble which is generated on a heater surface of 109 °C with a bulk water temperature of 97 °C (saturation temperature at point of bubble nucleation = 88 °C). While the general trend of the calculated curve agrees with the measurement a slightly higher surface temperature (approximately 115 °C) would give a better fit. Fig. 7 shows the length of the cylindrical bubble in another test (bulk liquid temperature 63 °C, saturation temperature 46 °C). Here fairly good agreement between measurement and calculation is indicated.

3. Superheat

3.1 Parameters and theoretical models

Till now experimental evidence indicates that - as predicted by theoretical models - liquid superheat is necessary to start boiling in organic liquids and water and to a much larger degree in liquid metals.

Available experimental data show a considerable disagreement and a wide range, too. There are many parameters which can influence the initial liquid superheat as there are (e.g.)

system pressure
heat flux
physico-chemical state of the liquid phase as
dissolved and suspended impurities or
gas, chemical agressivity
thermo-physical properties (especially the thermal conductivity)
liquid - solid interface characteristics as
surface roughness
adsorbed gas layer
oxide layer
thermo-physical properties
hydrodynamic conditions
gravity and radiation effects etc.

Experience shows that liquid-vapour phase transformation induced by heat transfer processes preferentially starts with nuclei formed at interfaces inside a system such as heater and container walls, free surfaces or liquid-gas interfaces of bubbles either entrained, injected or built up by adsorbed unsoluble gases. Contrary to this heterogeneous process the homogeneous nucleation takes place at random within homogeneous elements of volume of a phase, although this kind of transformation should be rather seldom because theoretically predicted nucleation frequencies corresponding to observed superheat values will be of a very small order.

Theoretical work mostly is based on the Volmer-Weber-Becker-Döring-theory (VWBD) [17,18] for nucleation of phase transformations, especially for the opposite effect of condensation of liquid out of supersaturated vapour. Including the decrease of concentration of embryos during a transition from phase 1 to phase 2 the nucleation frequency I becomes [19]:

$$I = z\, n_1\, s^{*} \left(\frac{-\, b \Delta G_v}{2\pi i^{*} kT}\right)^{1/2} \exp\left(-\frac{\Delta G^{*}}{kT}\right) \qquad (4)$$

with

b	pressure dependent parameter
ΔG_v	free energy per volume of the liquid phase with reference to the vapour phase
ΔG^*	free energy of formation of the nucleus
I	nucleation frequency per volume
i^*	number of molecules in the critical nucleus
k	Boltzmann constant
n_1	number of single molecules per volume phase 1
s^*	surface area of the nucleus
T	absolute temperature
z	collision frequency per area of vapour molecules with the surface of the nucleus

Equation (4) shows a sharp dependence of I on the critical value of the free energy ΔG^* which is necessary to generate a nucleus of the critical radius r^*. On the other hand this free energy is influenced by the surface tension σ and the supersaturation pressure ratio p_v/p_1, where p_v is the vapour pressure according to the temperature of the superheated liquid, p_1 is the liquid or system pressure. It is

$$\Delta G^* = \frac{16}{3} \pi \frac{\sigma^3}{p_1^2 \left(\frac{p_v}{p_1} - 1\right)^2} \qquad (5)$$

Although the VWBD-theory is successful in describing especially homogeneous condensation processes and with analogeous assumptions also the nucleation of crystalline phases, it fails when applied to the case of vapour bubble nucleation in boiling heat transfer. Nucleation frequencies and superheat observed in experiments are not yet explainable, even including the many parameters listed above. Comparing sodium to water the twice surface tension value of sodium leads to a factor 8 in the critical free energy or $2 \cdot 10^{-4}$ in the nucleation frequency rate I. A calculation of I using an experimentally reached superheat value of 300 °C at 1 atm system pressure for sodium results in $I \approx 10^{-1000000} \frac{1}{\text{sec cm}^3}$ whereas the experiment shows $I \approx 10^{-1} \frac{1}{\text{sec cm}^3}$

which illustrates the striking discrepancy between present day theory and the experimental evidence. In connection to the free energy level the influence of radiation on nucleation mechanisms starting the boiling process in liquid sodium has been investigated [20]. The consideration of several types of radiation results in the suggestion, that only sodium atoms centrally knocked on by fast neutrons would be able to deliver the required formation energy to create a critical vapour nucleus. In fact, even with this mechanism radiation induced nucleation seems probable only at saturation pressures of more than 10 atmospheres. There are also some other differences to bubble chamber processes, especially the better heat conduction in liquid metals and a larger value of the heat of vaporization, both prevent phase transformation at a lower energy level than pointed out above.

The degree of superheat in heterogeneous phase transformation processes decreases rapidly with an increasing number and volume of nucleation centers in form of gas or vapour embryos. In the case of ordinary liquids a solid interface normally is of such a roughness that enough nuclei exist as adsorbed gas or gas enclosed in cavities of various geometries called "active sites" for bubble generation. By degasing the surface by evacuation or by pressurizing the system, where the entrapped gas will be dissolved and the cavities are inactivated and penetrated by the liquid, also by polishing the surfaces it is possible to increase the values of initial superheat. In some longtime experiments a deactivation of nucleation sites has been observed, due to a degasing by the numerous generated bubbles.

The existence of such gas or vapour embryos depends especially on the wetting behaviour of the liquid-solid couple. The trapping mechanism has been analysed in more detail by Bankoff [21]. In Fig. 8 the influence of the liquid contact angle θ idealized is shown for a V-shaped cavity of the opening angle α. It can be seen that no gas will be trapped if $\theta \leq \alpha$ because the liquid will completely fill the bottom of the groove, Fig. 8a. If, as illustrated in Fig. 8b, $\theta > \alpha$ some gas will be enclosed in the bottom while the rest of the cavity fills with liquid. Due to the solubility of gas in the liquid or any chemical reaction between the trapped gas and the liquid the gas may disappear after some time and no longer be available as nucleation embryo.

Thermodynamic analysis of isothermal two-phase systems with spherical interface leads to the equilibrium equation of a bubble under surface tension forces (6) and to the Clausius-Clapeyron-equation (7) relating the pressure difference inside a bubble to the necessary superheat, even necessary in the case of a vapour or gas filled surface cavity for the growth of a nucleus to its critical size. From

$$p_v + p_g - p_l = \frac{2\sigma}{r^*} \tag{6}$$

and

$$\frac{dp}{dt} = \frac{\Delta h \, \rho_l \rho_v}{T (\rho_l - \rho_v)} \approx \frac{\Delta h \, p}{R \, T^2} \tag{7}$$

by integration and an approximation of the logarithm factor

$$T_v - T_s = \frac{2\sigma T_s}{\Delta h \, \rho_v \, r^*} \tag{8}$$

with

Δh	heat of vaporization
p	pressure
R	gas constant
r^*	critical radius of nucleus
ρ	density
σ	surface tension
T	absolute temperature

subscripts:

g	gas
l	liquid
s	saturation condition
v	vapour

A comparison of water as ordinary liquid to sodium as liquid metal coolant shows that because of the higher σ and T_s and the lower ρ_v for sodium a nucleus of the radius r^* results in a higher superheat than for water, both at the same system pressure.

In the case of sodium vapour bubble nucleation, however, there are some

other difficulties. At temperatures of more than 300 °C sodium is a well wetting liquid with a contact angle of almost zero to clean metal walls. The effect of this fact on gas-trapping in surface cavities already has been pointed out (see Fig. 8a,b), therefore sodium would fill cavities entirely and make them inactive. This wetting problem also is touched by a method developed by Holtz and Singer [22] who investigated the pressure temperature history of sodium cooled heat transfer systems. Considerations of wetting/non-wetting situations of surface cavities together with the assumption of an oxide layer covering the solid surface led to the conclusion that only partially penetrated cavities will act as nucleation sites at finite superheat as observed. Although there was some qualitative success with theoretical predictions the model needs a change from non-wetting to wetting inside a cavity basing on a chemical reaction between a surface-covering impurity layer and the liquid sodium, a mechanism which is quite unknown to date. The physico-chemical state of the sodium used for experimental comparisons had been neither measured nor discussed.

This leads to another important problem of superheat prediction in liquid sodium boiling. Contrary to water and ordinary liquids the alkali metals show high chemical aggressivity. Thereby thermodynamical processes which could be calculated rather simply will be superimposed by numerous physico-chemical reactions depending on the physico-chemical state of the whole system. Also the solubility of most gases in liquid alkali metals increases with increasing temperature as experiments show [23,24]. Therefore, in a heat transfer system where steadily cleaned sodium is passing the heated surfaces for long time, as in sodium cooled fast reactors, all possible active sites will be cleaned to a very large degree from any impurity layer or adsorbed and trapped gases. A flow induced concentration and temperature gradient will support this mass transfer process. This longtime effect has already been shown by Spiller et al. [25] in pool boiling experiments. So besides of the conditions of surface cavities also suspended impurities and dissolved or entrained gases as nucleation sites in the liquid metal may become more important, with respect to the maximum possible superheat till boiling starts, for longtime safety aspects in reactors.

3.2 Experimental results

Published experiments on sodium and potassium wall superheat measurement show widely spread values [8,22]. This fact is not very surprising

because of the numerous influences pointed out in 3.1, and because it is not possible to exclude all parameters except one. Especially investigations with variation of the physico-chemical state until to date are not reported.

For pool boiling of sodium superheat values of 0 °C up to 330 °C [25,26,27,28] have been found. Also in natural and forced convection loop experiments superheat values stay within a range of 50 °C [13] to 220 °C [29,30] except for one experiment done at Ispra - where stagnant potassium under very clean conditions reached maximum wall superheat values up to 800 °C [13] - the purity of the liquid metal and the amount of dissolved gases is not very well known.

Experimental work at Karlsruhe aims at clearing up some physico-chemical parameters influencing the liquid sodium superheat. First experimental runs in absence of any gas atmosphere with very carefully degased sodium and evacuated apparatus have been done. The experimental arrangement is shown in Fig. 14. The results of nearly 150 runs are plotted in Fig. 9 compared to theoretically calculated critical radii of nuclei according to equation (6). It can be seen that the superheat values fall into a narrow range decreasing with increasing saturation temperature, as the theory predicts, and there has been no indication of a time dependent effect such as discussed in 3.1. Because of the unknown surface conditions inside the heated part of the apparatus no correlation of the experimental results to the theoretical curves can be stated. More detailed experiments must follow.

Another pool boiling experiment facility has been constructed with special emphasis on wall effects. An artificial cavity - until to date a cylindrical hole of 0,4 mm diameter and 2 mm depth - is positioned in the center of a "hot finger" in a flat polished surface. A first experiment carried out after a cleaning and instrumentation testing period showed a superheat value of 35 °C at a saturation temperature T_s = 572 °C.This corresponds to a critical bubble diameter of 0,4 mm, calculated from equation (8). Compared to the cavity diameter there is a surprisingly good agreement. However, since only few test runs have been made, this cannot yet be taken as proof of any theory.

Generally it can be stated that to date an exact theoretical prediction of liquid superheat especially for liquid metal bubble nucleation is

impossible. Although there are some very good agreements between some experiments and some theories, on the other hand there are always results stating unexplainable discrepancies. To understand the influence of the various parameters on superheat and nucleation mechanism much more and detailed theoretical and experimental work will be necessary.

4. Recondensation

Phenomena and Effects

After having discussed nucleation and growth of vapour bubbles in fast reactors we shall now consider the recondensation. When the bubble grows further it will reach colder (non-heated) sections of the coolant channels and finally enter a plenum in which the temperature is less than the saturation temperature. This is indicated as phase 4 on Fig. 1. This may be called the heat-pipe-phase. The liquid layer on the fuel rod surface will continue to produce vapour which will condensate on the colder surface. Thus the fuel rod will still be cooled.

When the liquid layer dries out, there are two consequences to be considered:

(1) Due to the lack of cooling the fuel rod temperature will start to rise and may reach the melting point of the cladding.

(2) Due to the reduced vapour production rate the pressure will drop and the liquid will reenter the coolant channel.

Whether the fuel rod assembly will be destroyed due to melting before it is wetted again by the liquid is still unresolved. This will depend on the mode of reentry of the liquid and on the specific power of the fuel.

There are two basic modes of reentry. The liquid may enter the coolant channel in a similar way as it was ejected, namely as a liquid slug with a welldefined liquid-vapour interface. In this case liquid hammer effects must be expected with very high pressure pulses of short duration. The maximum pressures at the moment of collapse of condensating vapour bubbles are much higher than the vapour pressure (which is the maximum pressure during boiling). This has been demonstrated in sodium boiling and recondensation experiments as shown on Fig. 10 and was also pre-

dicted by theory [8,10]. However, other modes of reentry are possible and even more likely: small quantities of liquid may come into contact with hot surfaces prior to the bulk of the liquid. In this case, vapour will be produced which would slow down the liquid slug and lead to repeated ejections, but extremely high pressures will not occur in this case.

Sooner or later the fuel rod assembly will fail in either case unless the defect is detected and the reactor is shut down. Although this would cause significant local damage, only propagation of the failure might have public hazard implications. The time available to take corrective action will depend on the rate of failure propagation. Fast propagation of fuel failure over a large number of fuel elements must be prevented. The rate of propagation will depend on the mode of reentry. Apparently, mechanical deformation of the core structure by liquid hammer effects would be the fastest failure propagation mechanism. Therefore, the liquid hammer mode of reentry is usually given most attention [8, 31, 32] although it is by no means the most probable mode.

5. Experimental Program

An extensive research program was established für the experimental investigation of boiling phenomena and related background information for various liquids and in particular for sodium. Some of the experiments which are closely related to the subjects covered in this paper shall be described briefly.

5.1 Ejection and Recondensation

Fig. 11 shows the interrelationship of four series of experiments which were designed to provide detailed knowledge of the boiling, ejection and recondensation phenomena and to permit reliable predictions of the events in a fast sodium cooled reactor under certain accident conditions. The Ejection Simulation Experiment in single rod configuration has proven to be a useful tool for establishing the theoretical model. Its results are also used to check the calculations in a simple geometry (see Fig. 6 and 7). The test loop (as shown on Fig. 12) is filled with highly purified and degased water. The test section consists of a glass tube with a central electrical resistance

heater. The hydraulic diameter was chosen according to fast reactor design. The temperature of the test section is controlled by means of a glycerine thermostat circuit prior to the test. Bulk superheat values of 20 ^{o}C are generally achieved at system pressures of some 10 mm Hg. At heat fluxes up to 60 W/cm^2 single bubble ejection occurred similar to the case with sodium, while at higher heat fluxes (over 100 W/cm^2 were reached) the "selfpressurization" was insufficient to prevent formation of series of bubbles. Pressure and temperature sensors are indicated on Fig. 12. High speed movies are taken from the ejection process.

Design of a similar test section is underway for the Bundle Ejection Simulation Experiment. A resistance type heater bundle with 19 rods is planned for the first step. This will permit optical and instrumental observation of the influence of a bundle geometry upon fluid flow as compared to the single rod case.

The Ejection Simulation Experiment facility will also be used to investigate the recondensation problem. Especially, the flow pattern of the reentrant liquid will be investigated by optical observation. Some modifications may be necessary to get better analogy to the reactor conditions during this phase.

Complementary to the water tests experiments will be carried out with sodium. The general arrangement of the Sodium Boiling Loop is shown on Fig. 13. The stainless steel test section is heated by an oil cooled high frequency power supply. The whole loop is contained in a nitrogen filled cell for safety reasons. Both the loop and the high frequency heated test tube have operated successfully in separate tests. With water maximum heat fluxes of 700 W/cm^2 have been achieved. Special emphasis is layed on the control of the purity of the sodium. A special sodium destilling device was developed for taking representative samples of the sodium for wet chemical analysis. The loop is connected to a large sodium facility (used for technological test) including a sodium purification plant. Hence the test sodium will have an impurity content representative of large scale facilities such as a reactor. The information supplied by pressure, temperature and flow sensors during the tests will be used to check and to improve the theoretical model.

The Sodium Boiling Test Bundle was conceived to simulate reactor

conditions as closely as possible out of pile. Because of the difficulties of instrumentation in a closely packed bundle of 169 heater rods of 6 mm diameter this experiment is not expected to provide information about the details of the ejection and recondensation process. However, this experiment shall provide information about the mechanical effects of sodium boiling with all its consequences in a typical fast reactor fuel element. Therefore, the test bundle will be surrounded by six other bundles of similar geometry and composition as in the reactor. Digital analysis of the transient temperature rise in the bundle indicates that with commercially available heater rods a relatively flat temperature profile can be achieved in the bundle to superheat a sufficient quantity of sodium without excessive energy losses to the environment. The temperature distribution will approach closely the reactor case for loss of flow situations so that this experiment will allow confident predictions as to reactor conditions.

5.2 Sodium Superheat

The experimental research program on sodium superheat is especially concentrated on the influence of physico-chemical effects such as

solubility of inert gases above 600 °C
sodium conditions (oxide concentration) and
wall condition (artificial cavities).

A first experimental arrangement is shown in Fig. 14. Inside a test chamber the sodium will be superheated by radiation heating in absence of any gas atmosphere. To prevent natural convection and heat transfer the chamber is positioned on the top of the apparatus. By steadily pulling at the stainless steel bellow in the lower part the pressure can be varied and a certain amount of superheat will be reached. Some time after pressure decrease the nucleation will take place and the liquid metal flashes out of the hot chamber. For registration of the whole run thermocouples and pressure pick-ups are installed, the signals are fixed by an UV-oscilloscript because of the high velocity requirements. Fig. 14 also shows the general distribution of the temperature inside the facility and the position of the two piezoelectric quartz pressure transducers and the tube connecting the apparatus to a seperate heated Bourdon-tube to measure the static pressure inside the test section

before any nucleation.

The sodium contents can be changed. Thus a controlled variation of the oxide concentration and dissolved gases as helium or argon is possible.

Instead of decreasing the pressure to obtain superheated liquid in another facility at constant pressure the temperature in a "hot finger"-like test area is raised until nucleation starts. The test section is shown in Fig. 15. A flow diagram of the whole facility is shown in Fig. 16. The heavily drawn lines indicate sodium containing components. To reach controlled sodium conditions, especially a certain oxide concentration, the test section is arranged as part of a natural convection loop with a cold trap and a hot trap. Thus the circulating hot sodium cleans the test area by mass transport of impurities either to the cold trap or to the hot trap. The cold trap in the part of the lower temperature is filled with stainless steel mesh work whereas the hot trap contains zirconium chips. Each one of the traps is bypassed during operation of the other one to complete the circulation loop in each cleaning phase. The facility is completed by an argon covergas supply with a NaK-cleaning pool and a vacuum system with liquid nitrogen trap. The power supply and the control instrumentation mainly in form of 50 thermocouples are not shown.

Several series of experiments will be carried out with a variation of the sodium conditions as well as the geometry of the artificial surface roughness already mentioned. A special emphasis also is laid on the time dependence of superheat in a long time program of repetition of the same experimental run.

Summary

a) The mechanism of single channel ejection is understood quite well. The theory has been checked against experimental results with water and liquid metal successfully.

b) The most important and at same time the least known parameter so far is the liquid superheat at the instant of bubble nucleation. Predictions on the basis of present day theories fail. Important influences upon superheat - physico-chemical state and liquid-solid interface effects - will be investigated in the current research program.

c) The fluid flow pattern in rod bundle geometries will be studied with water and sodium. Thus reliable predictions to reactor conditions will be possible.

d) The two-phase flow behaviour and mechanical effects during reentry are particularly related to reactor safety. Research work must be concentrated in these problems in the future.

References

[1] R.C. Noyes, H. Lurie, A.A. Jarrett:
The Development and Growth of In-Core Voids due to Boiling during Fast Reactor Transients.
ANL-7120, October 1965.

[2] A.M. Judd:
Loss of Coolant Accidents in a Large Sodium Cooled Fast Reactor. ANL-7120, October 1965

[3] G. Friz:
Coolant Ejection Studies with Analogy Experiments.
ANL-7120, October 1965.

[4] M. Fischer, W. Häfele:
Shock Front Conditions in Two-Phase Flow Including the Case of Desuperheat. ANL-7120, October 1965.

[5] D.R. MacFarlane:
An Analytic Study of the Transient Boiling of Sodium in Reactor Coolant Channels. ANL-7222, June 1966.

[6] R.C. Noyes, J.G. Morgan, H.H. Chappel:
TRANSFUGUE-I, A Digital Code for Transient Two-Phase Flow and Heat Transfer. NAA-SR-11008, July 1965.

[7] General Electric Co.:
Fast Ceramic Reactor Development Program. Eighteenth Quarterly Report. GEAP-5158, April 1966.

[8] W. Peppler, E.G. Schlechtendahl, G.F. Schultheiss, D. Smidt:
Sodium Boiling and Fast Reactor Safety. KFK-612, June 1967.

[9] E.G. Schlechtendahl:
Die Ejektion von Natrium aus Reaktorkühlkanälen.
Nukleonik 10, Heft 5, 1967.

[10] A.M. Judd:
Boiling and Condensation of Sodium in Relation to Fast Reactor Safety.
Conference Internationale sur la Surete des Reacteurs a Neutrons Rapides, September 1967.

[11] L.M. Milne-Thomson:
Theoretical Hydrodynamics.
MacMillan + Co., London, 1962.

[12] R. Cole, H.L. Shulman:
Bubble Growth Rates at High Jakob Numbers. Int. J. Heat Mass Transfer, Vol. 9, pp. 1377 - 1390, 1966.

[13] K.H. Spiller, G. Grass, D. Perschke:
Überhitzung und Einzelblasenejektion bei der Verdampfung von stagnierenden Flüssigmetallen.
Atomkernenergie, Vol. 12, Heft 3/4, 1967.

[14] K. Dumm, H. Mausbeck, W. Schnitker:
Experimental and Theoretical Investigations of Sodium-Water Reactions in Tubes. CREST, Meeting of Specialists on Shock Structure Interactions in a Reactor, ISPRA, June 1966.

[15] R.G. Deissler:
Investigations of Turbulent Flow and Heat Transfer in Smooth Tubes Including the Effects of Variable Fluid Properties.
Trans.ASME 73, 101 (1951).

[16] G. Grass, H. Kottowsk, R. Warnsing:
Das Sieden von flüssigen Alkalimetallen.
Atomkernenergie, Vol. 12, Heft 3/4, 1967.

[17] M. Volmer, A. Weber:
Z. Phys. Chem. 119 (1925) 277

[18] R. Becker, W. Döring:
Ann. Phys. [5] 24 (1935) 719

[19] J.H. Hollomon, D. Turnbull:
Progress in Metal Physics, Vol. 3, pp 333 - 388

[20] K.T. Claxton:
The Influence of Radiation on the Inception of Boiling in Liquid Sodium.
Conference Internationale sur la Surete des Reacteurs a Neutrons Rapides, Sept. 1967.

[21] S.G. Bankoff:
A.I. Ch. E. J. 4, 24 (1958)

[22] R.E. Holtz, R.M. Singer:
On the Superheat of Sodium at Low Heat Fluxes.
ANL-7383, November 1967.

[23] S.K. Dhar:
Solubility of argon in sodium. ANL-6800, pp. 183 - 187

[24] S.K. Dhar:
Solubility of krypton in liquid sodium. ANL-6900, pp. 125 - 127

[25] K.H. Spiller, D. Perschke, G. Grass:
Überhitzung und Einzelblasenejektion von stagnierendem Natrium.
(to be published)

[26] B.S. Petukhov, S.A. Kovaler, V.M. Zhukov:
Study of sodium boiling heat transfer. Proc. of 3. Int. Heat Transfer Conf., Chicago, August 1966, Vol. V, pp. 80 - 91

[27] R.C. Noyes:
Boiling studies for sodium reactor safety, Part I.
NAA-SR-7909, 1963

[28] P.J. Marto, W.M. Rohsenow:
Effects of surface conditions on nucleate pool boiling of sodium. Trans.ASME, Ser.C., Journ.Heat Transfer 88, 1966, No. 2, pp. 196 - 204

[29] H.W. Hoffmann, A.I. Krakoviak:
Convective boiling with liquid potassium. Heat Transfer and Fluid Mechanics Institute, Univ. of California, Berkeley, 10 - 12 June 1964, Stanford University Press, pp. 19 - 37.

[30] H.W. Hoffmann, A.I. Krakoviak:
Forced convection saturation boiling of potassium at near-atmospheric pressure. Proc. of 1962 High-Temp. Liquid Metal Heat Transfer Technology Meeting, BNL 756, 1963, pp. 182 - 203

[31] K. Gast, E.G. Schlechtendahl:
Schneller Natriumgekühlter Reaktor Na 2. KFK 660, EUR-3706 d, Oktober 1967.

[32] E.G. Schlechtendahl, M. Cramer, K. Gast, G. Heusener, W. Merk, W. Schikarski, E. Schönfeld, D. Smidt:
Safety Features of a 300 MW_e Sodium Cooled Fast Breeder Reactor (Na 2). KFK 611, June 1967.

Fig.1: Model of Coolant Channel Ejection

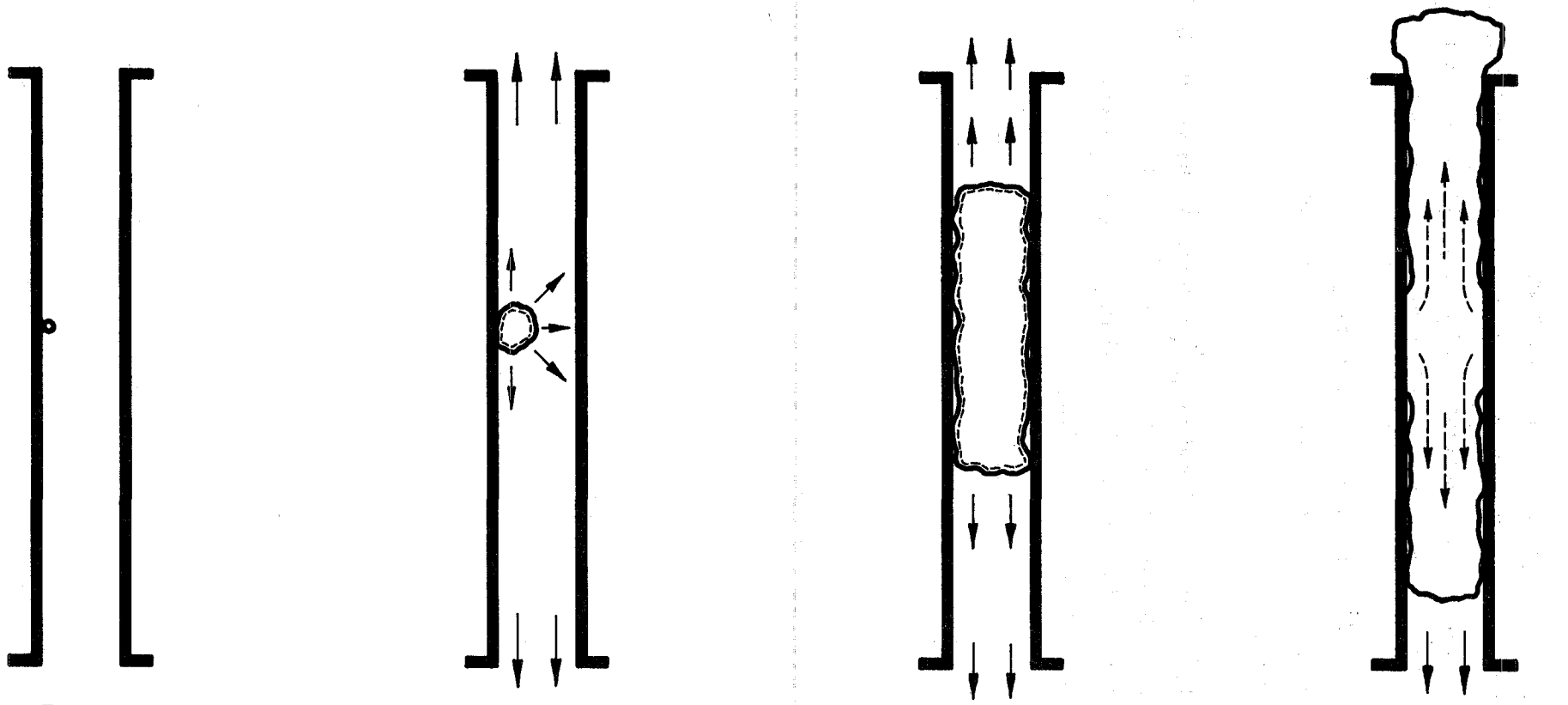

Phase 1
Superheat and
Bubble Nucleation

Phase 2
Spherical Bubble

Phase 3
Cylindrical Bubble

Phase 4
Heat Pipe Phase

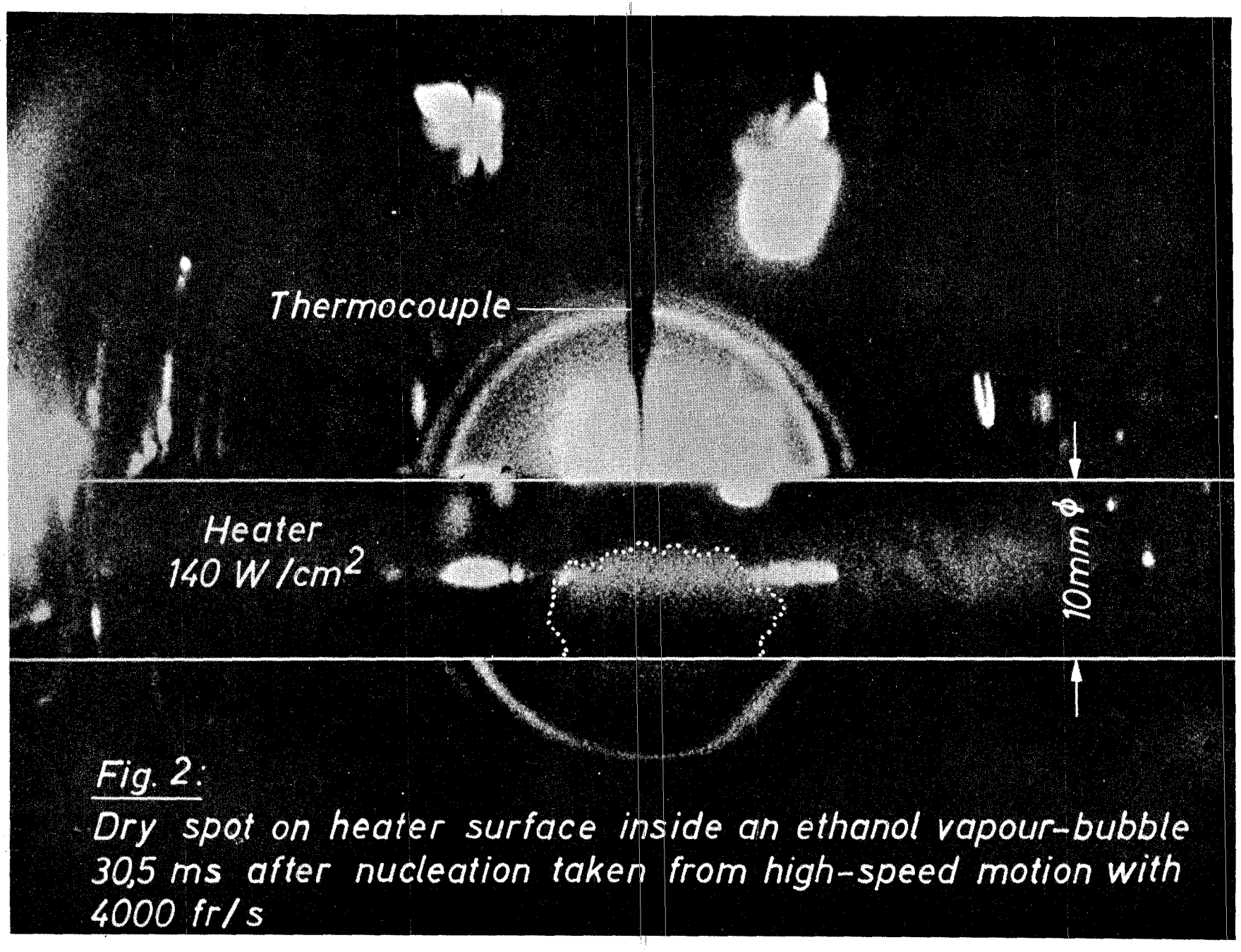

Fig. 2:
Dry spot on heater surface inside an ethanol vapour-bubble 30,5 ms after nucleation taken from high-speed motion with 4000 fr/s

Fig. 3 Liquid Layer Thickness

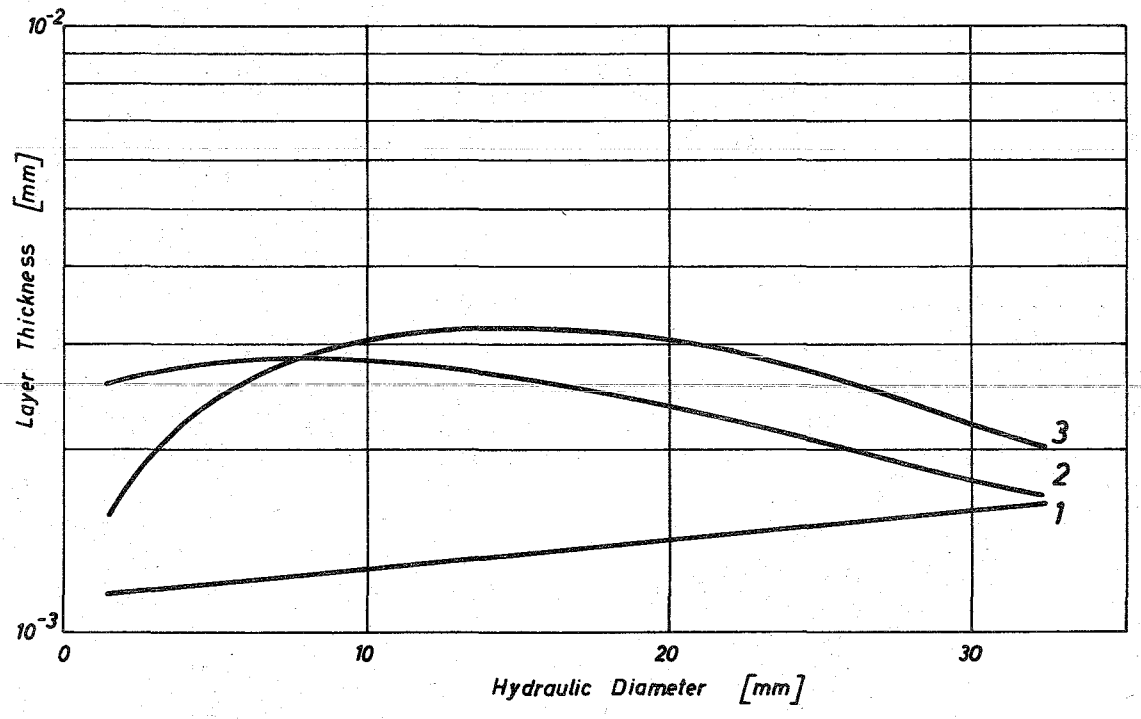

1 mass balance

2 energy balance

3 laminar sublayer thickness

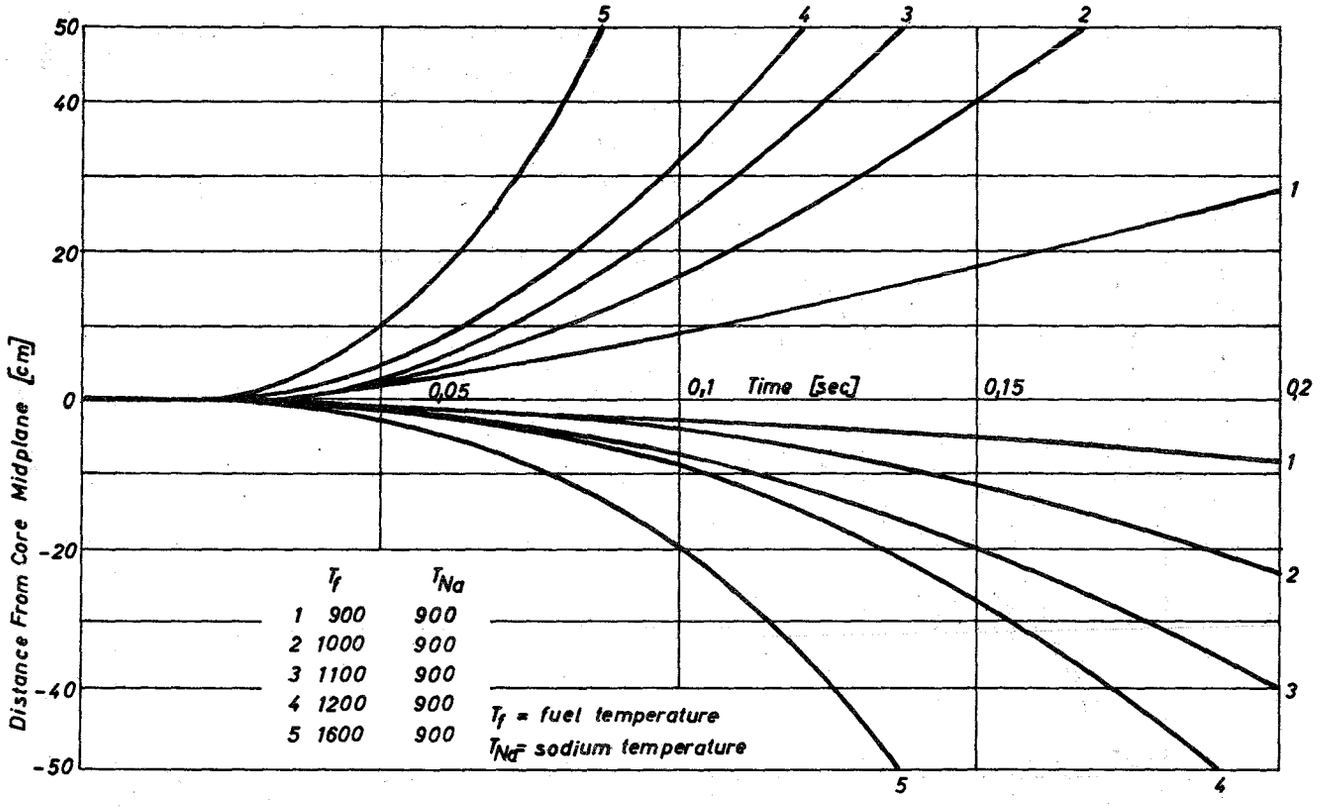

Fig. 4: Sodium ejection with 20° C liquid superheat

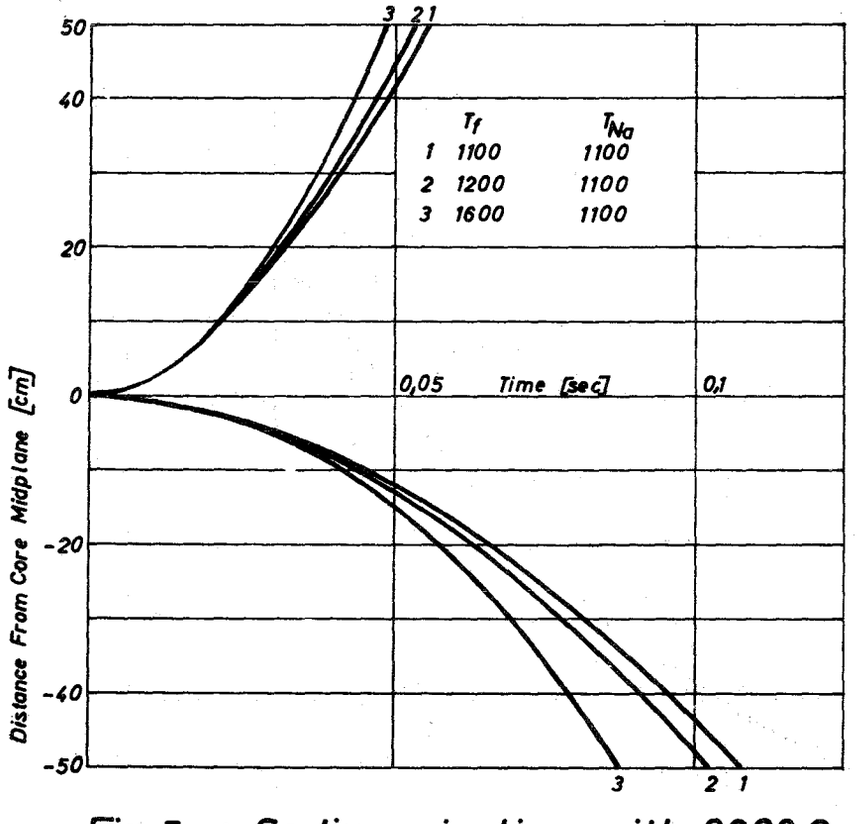

Fig. 5 : Sodium ejection with 220° C liquid superheat

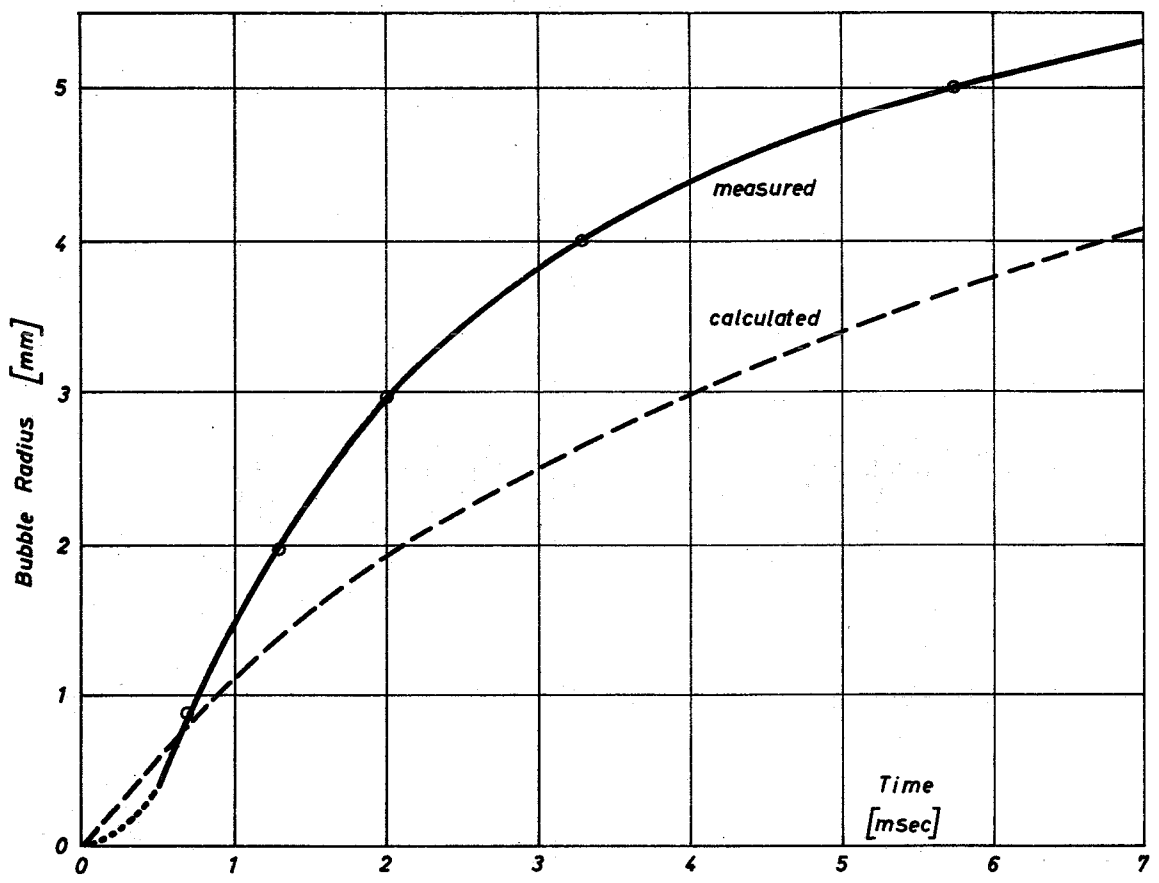

Fig. 6 : Radius of Spherical Bubble

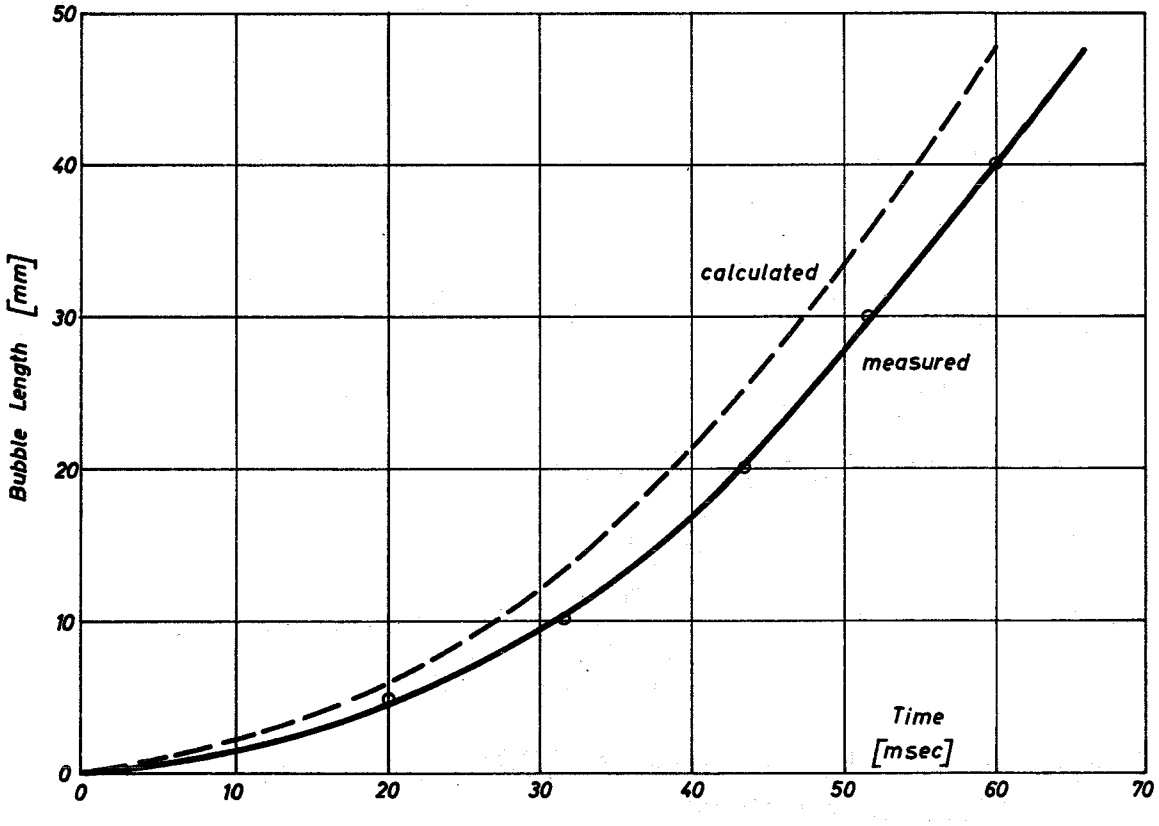

Fig.7 : Lenght of Cylindrical Bubble

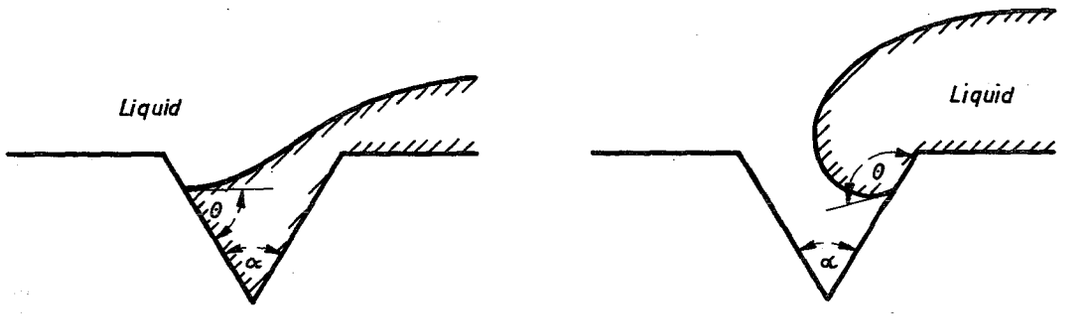

a) $\theta \leq \alpha$ b) $\theta > \alpha$

θ = Contact Angle
α = Opening Angle

Fig. 8 : Liquid entering a Cavity at Different Contact Angles

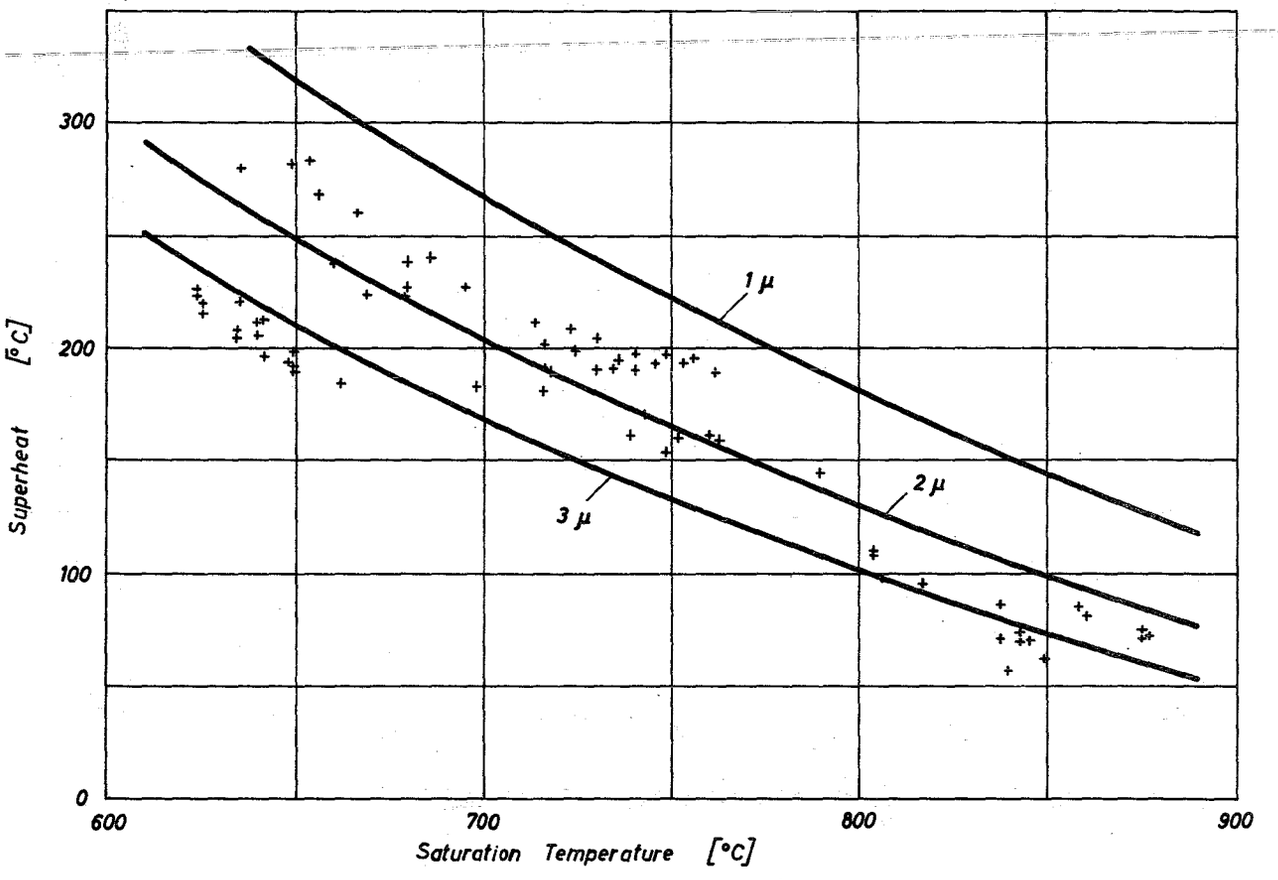

Fig. 9 : Sodium Superheat at Different Saturation Temperature

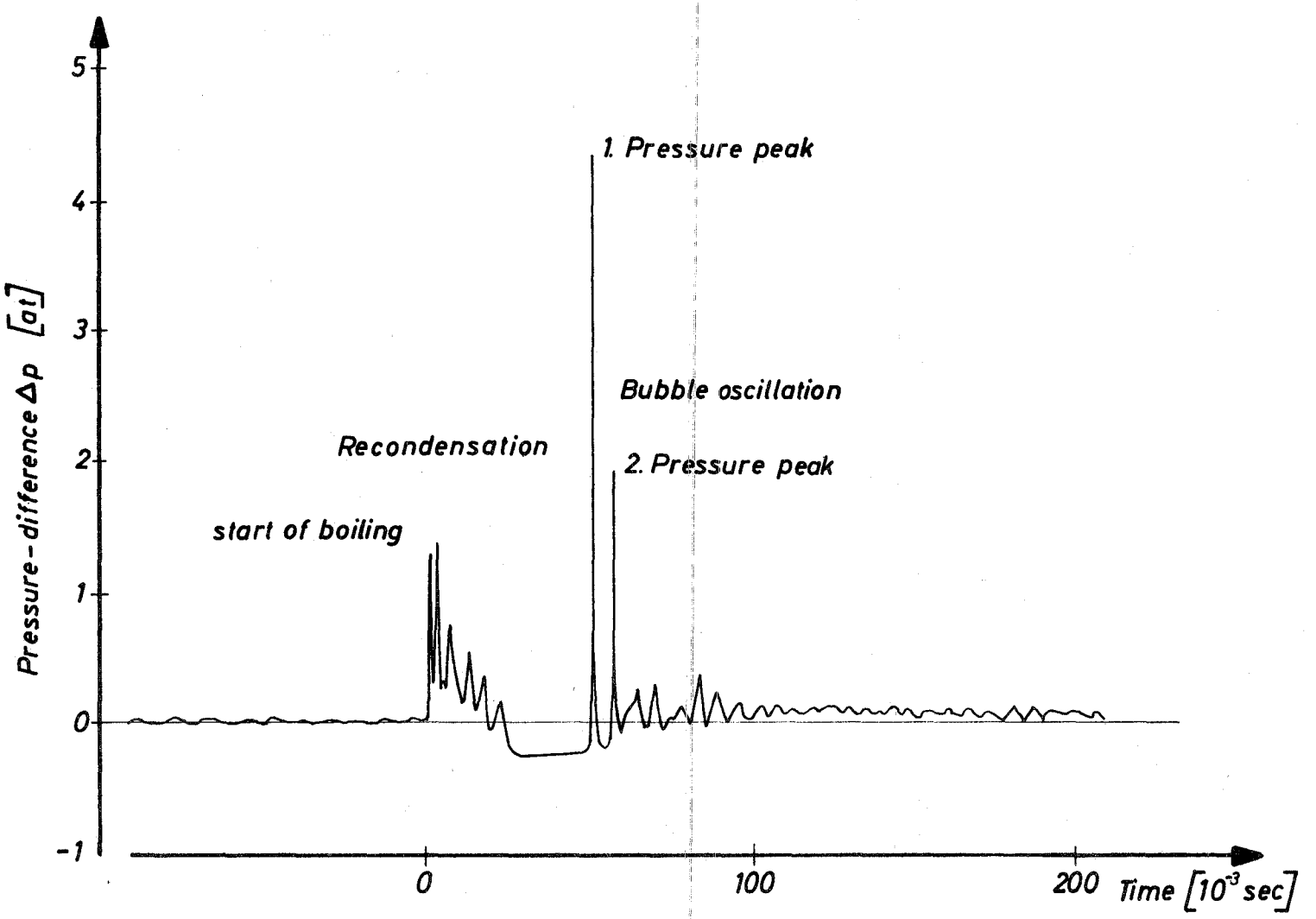

Fig. 10 Pressure - difference $\Delta p = p_{abs} - p_{system}$ vs time of a sodium boiling and recondensation experiment

Fig. 11 : Ejection and Recondensation Experiments
Flow of Information

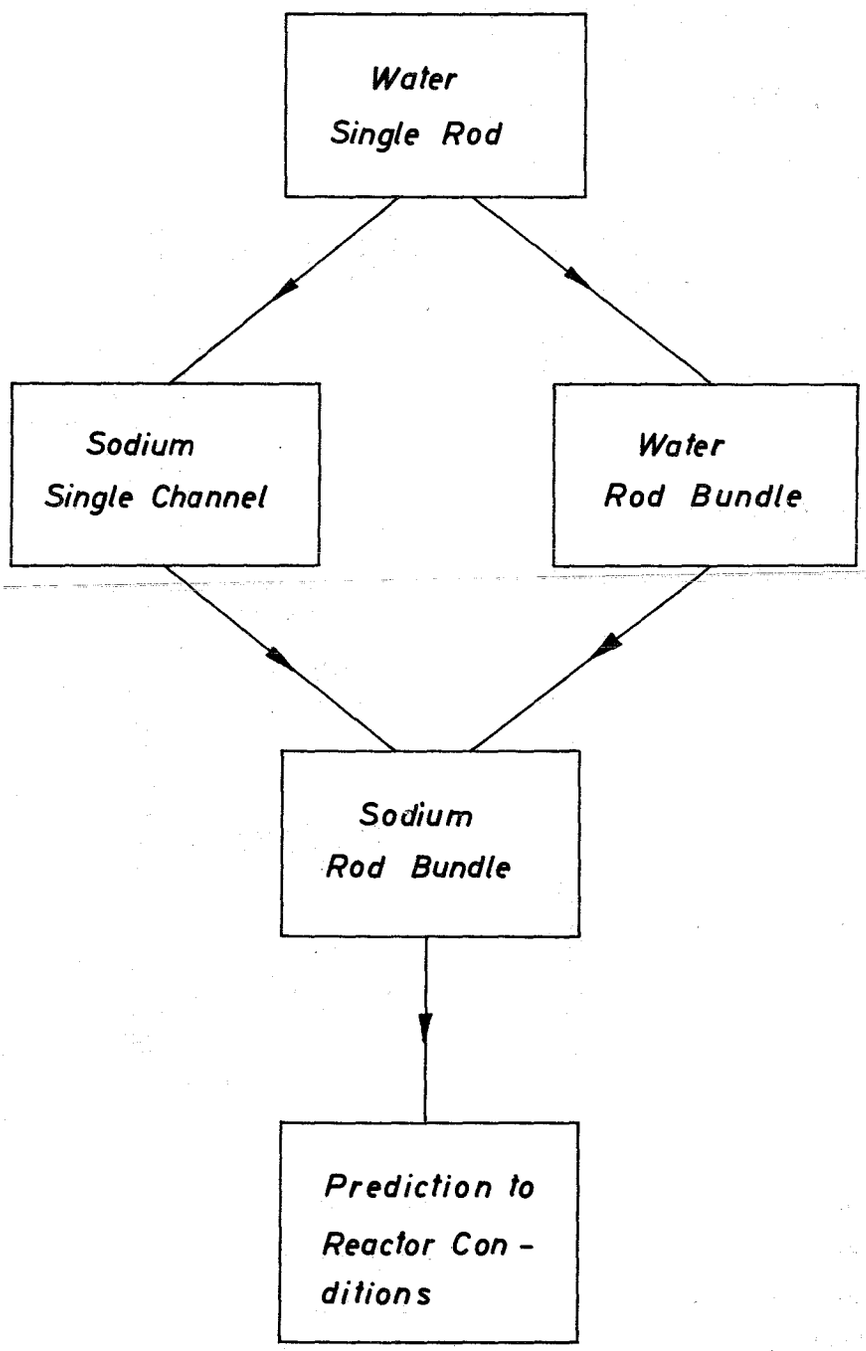

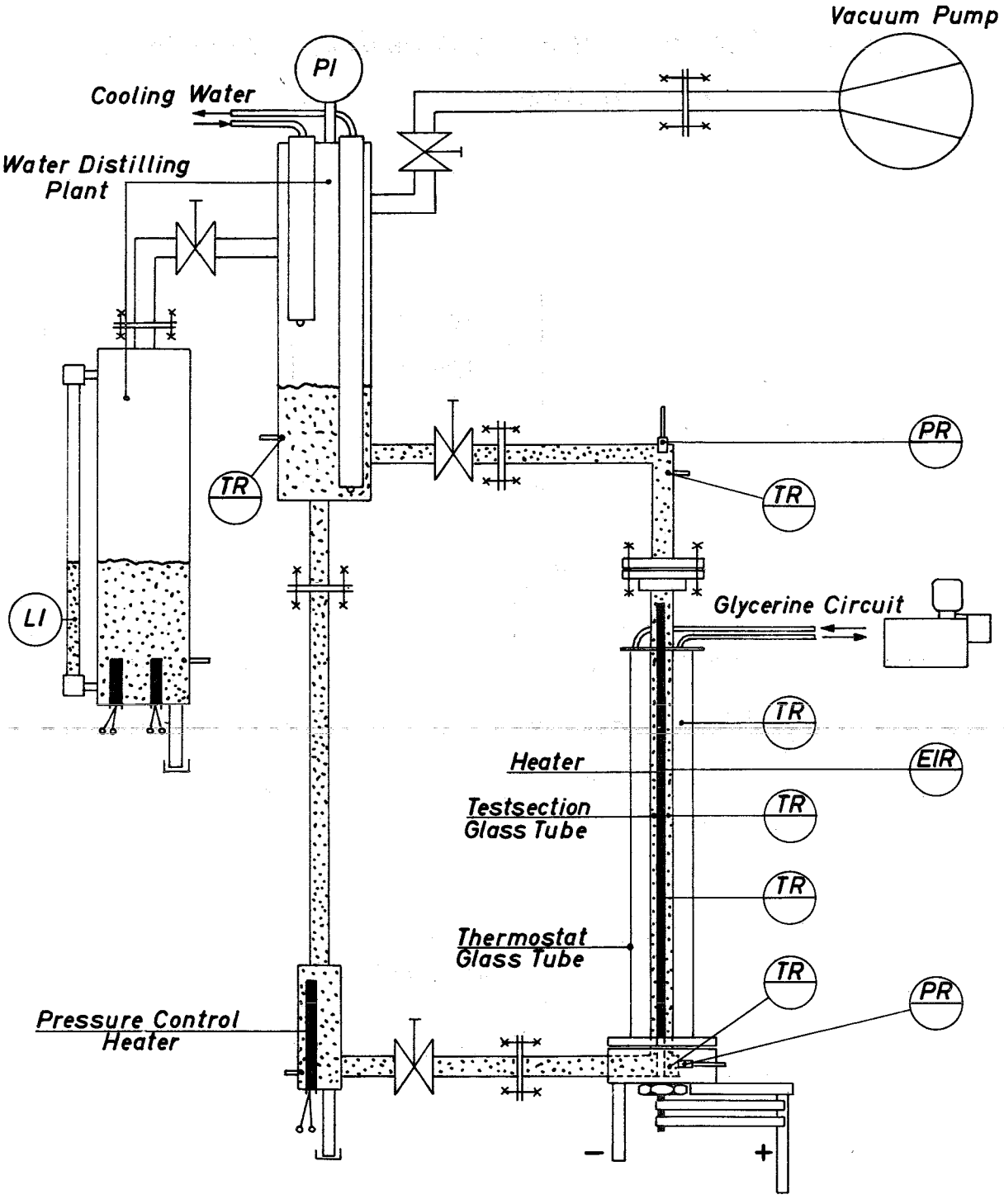

E Power
L Level
P Pressure
T Temperature

I Indication
R Registration
Local Indication
Indication or Registration on Operator Desk

Fig. 12: Ejection Simulation Experiment Water Test-Loop

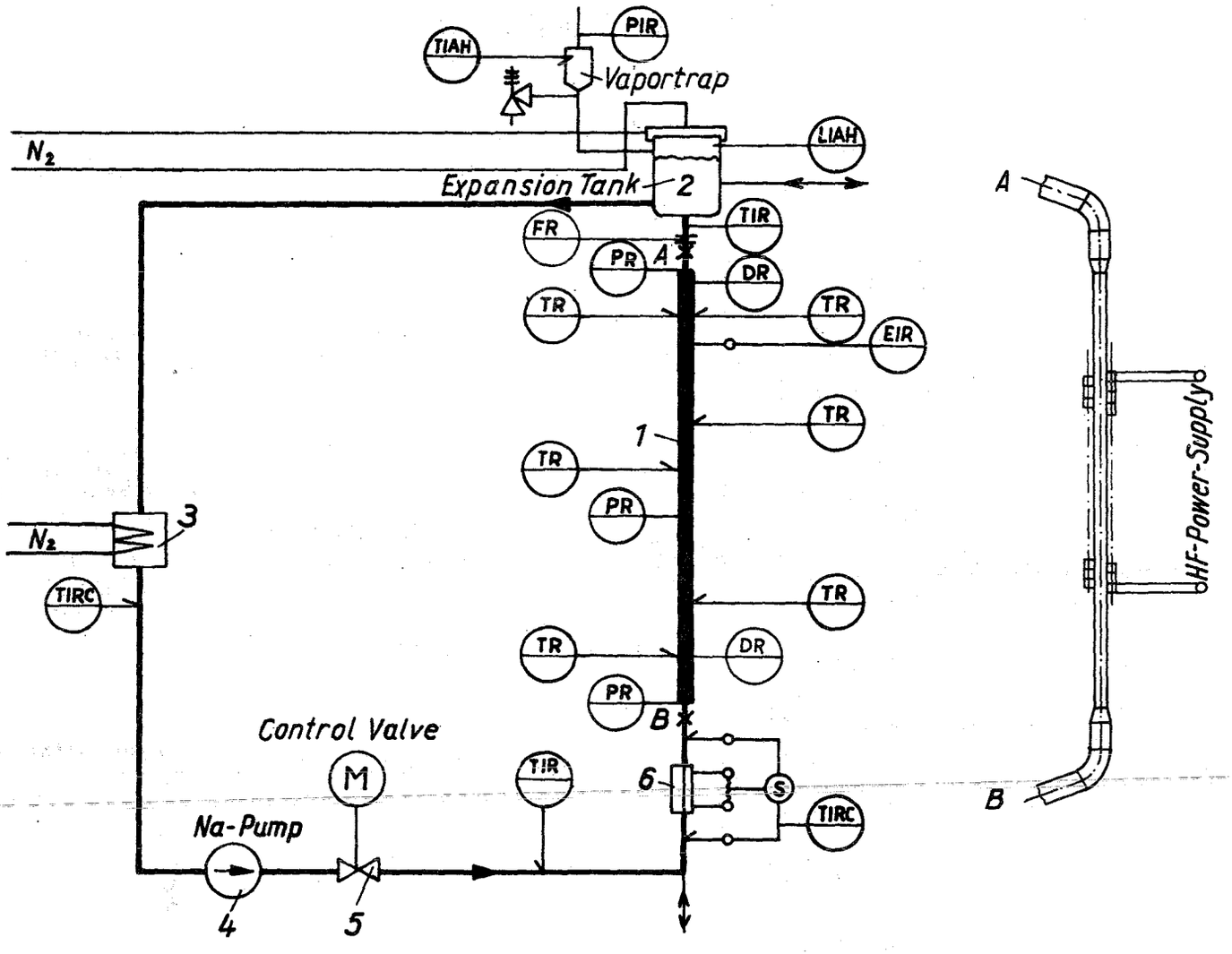

Power	E	Level	L
Temperature	T	Indication	I
Flow	F	Registration	R
Pressure	P	Alarm[High-low]A[HL]	
Density	D	Control	C

◯ Indication Local

⊖ Indication or Registration on Operator Desk

Sodium-Loop

Testsection

Fig. 13: Na2 Loop

Fig. 14 : Sodium Superheat Experiment

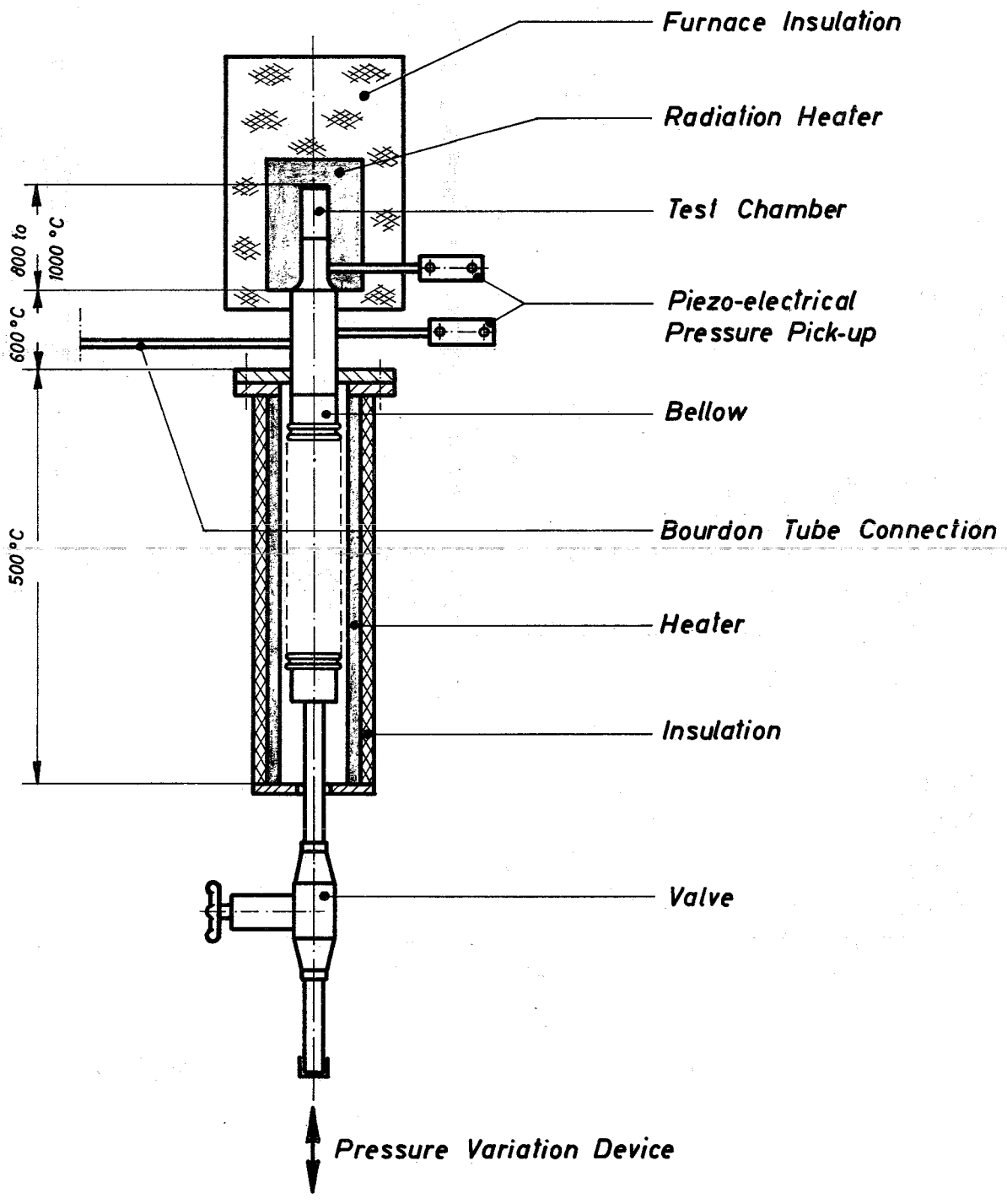

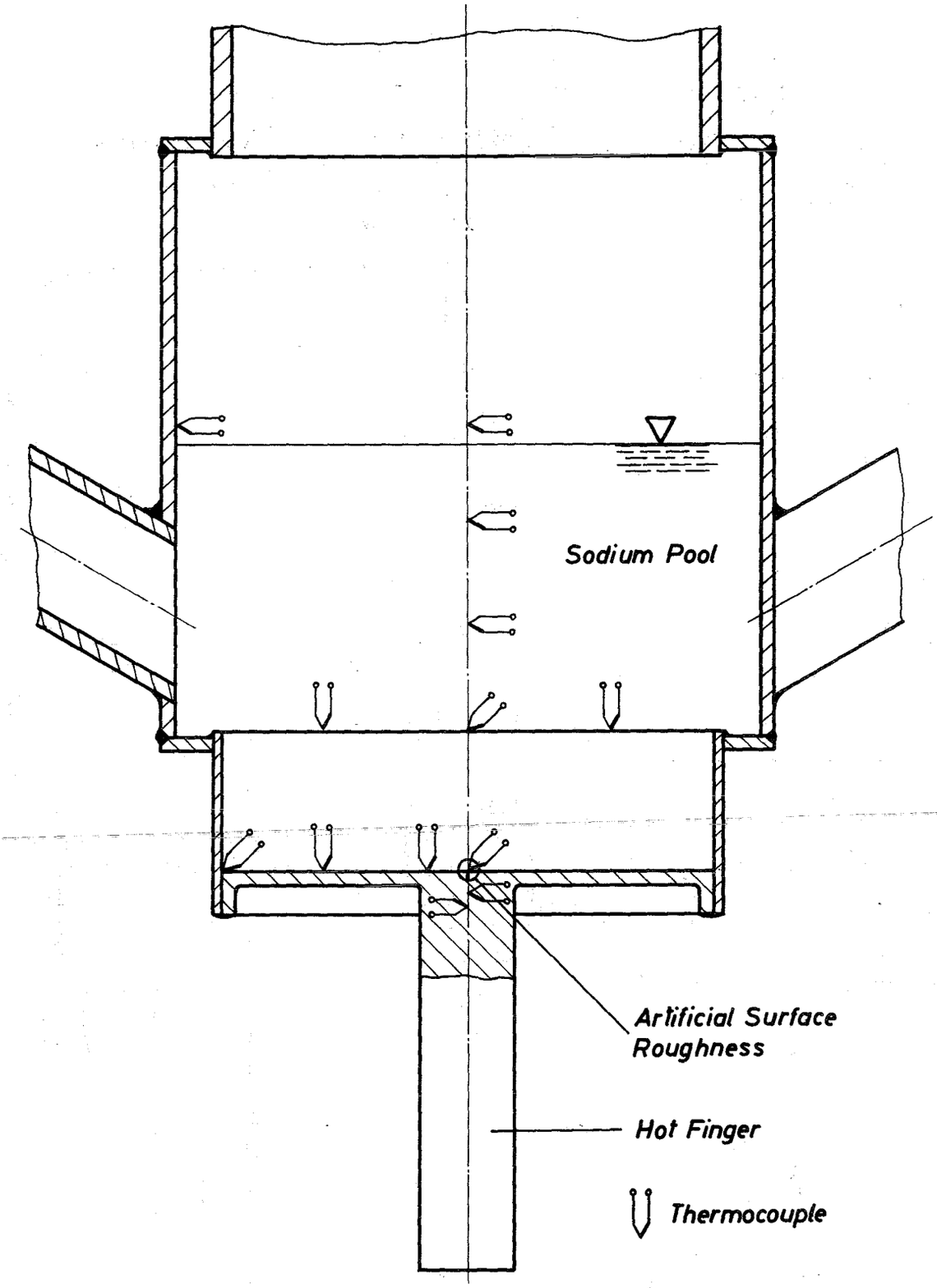

Fig. 15: Test Section of Wall Superheat Experiment

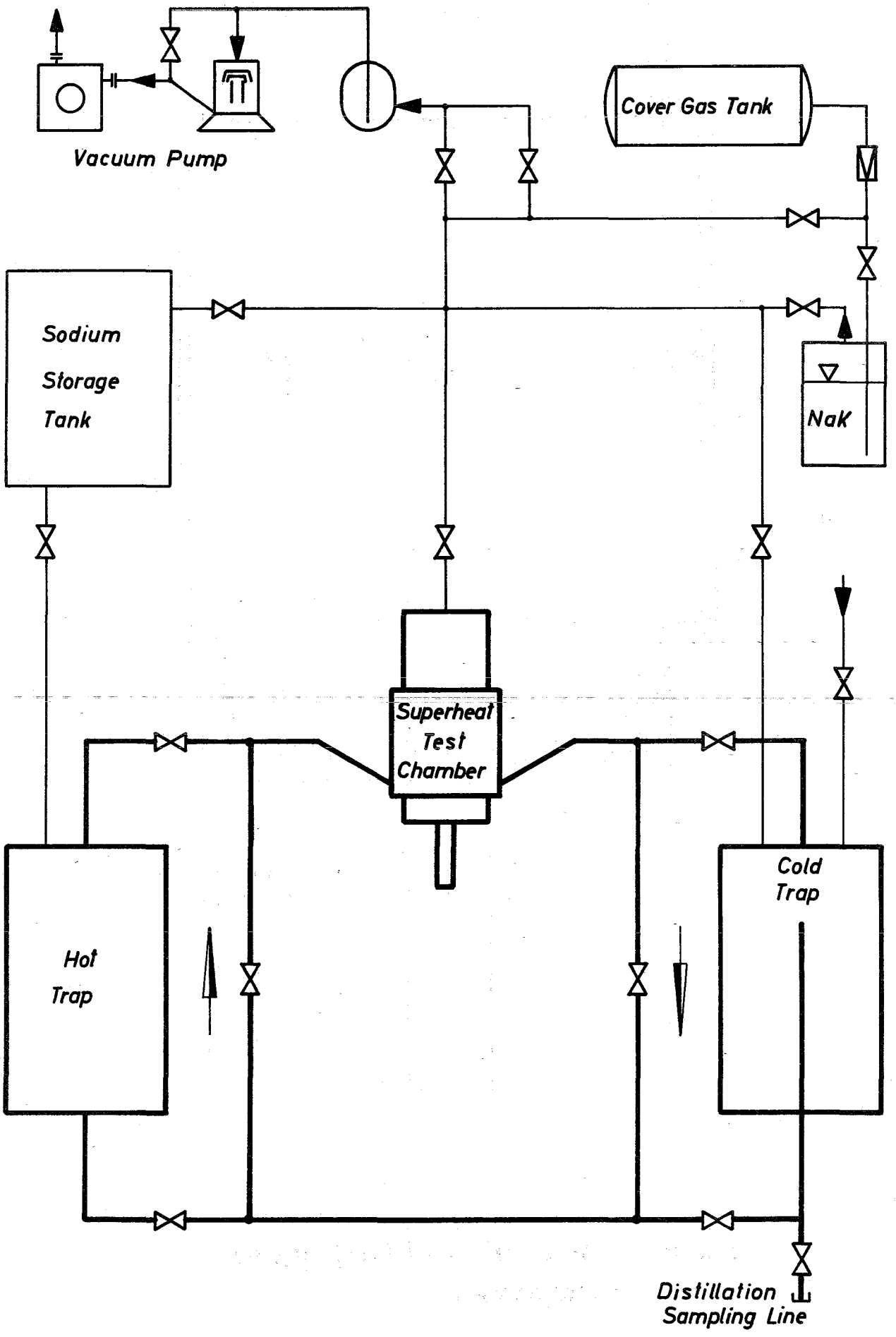

Fig. 16: Flow Diagram of Wall Superheat Experiment